THE ANATOMICAL RECORD 294:1685–1697 (2011)

Altered Expression of Tyrosine Hydroxylase in the Locus Coeruleus Noradrenergic System in Citalopram Neonatally Exposed Rats and Monoamine Oxidase A Knock Out Mice

JUNLIN ZHANG,[1] RYAN D. DARLING,[1] IAN A. PAUL,[2] KIMBERLY L. SIMPSON,[1,2]* KEVIN CHEN,[3] JEAN C. SHIH,[3,4] AND RICK C.S. LIN[1,2]

[1]Department of Anatomy, University of Mississippi Medical Center, Jackson, Mississippi
[2]Department of Psychiatry and Human Behavior, University of Mississippi Medical Center, Jackson, Mississippi
[3]Department of Pharmacology and Pharmaceutical Sciences, University of Southern California, Los Angeles, California
[4]Department of Cell and Neurobiology, University of Southern California, Los Angeles, California

ABSTRACT

In rodents, noradrenergic (NE) locus coeruleus (LC) neurons are well known to express tyrosine hydroxylase (TH) immunoreactivity. However, due to its very low enzyme activity, NE cortical fibers do not typically express TH immunoreactivity, thus dopamine-β-hydroxylase (DBH) immunoreactivity is commonly utilized as a marker for NE cortical fibers. In this study, we performed double and/or triple immunofluorescent staining using antibodies against TH, DBH, and/or norepinephrine transporter (NET) to investigate the altered NE TH expression of cortical fibers in citalopram (CTM)-exposed rats and monoamine oxidase (MAO) A knock out (KO) mice. We have noted the following novel findings: (1) neonatal exposure to the selective serotonin reuptake inhibitor (SSRI) CTM enhanced NE TH immunoreactive fibers throughout the entire neocortex, and a few of them appeared to be hypertrophic; (2) slightly enhanced NE cortical TH immunoreactive fibers were also noted in MAO A KO mice, and many of them revealed varicosities compared with the rather smooth NE cortical TH immunoreactive fibers in wild-type (WT) mice; (3) LC dendrites of MAO A KO mice exhibited beaded morphology compared with the smooth LC dendrites in WT mice. Our findings suggest that both genetic and environmental factors during early development may play a critical role in the regulation and proper function of NE TH expression in the neocortex. Anat Rec, 294:1685–1697, 2011.

Key words: norepinephrine; tyrosine hydroxylase; monoamine oxidase; neonates; antidepressants; knock out mice

Grant sponsor: Natural Institutes of Health; Grant number: MH39085.

Grant sponsor: Natural Institutes of Health; Grant number: EUREKA MH084194.

*Correspondence to: Dr. Kimberly L. Simpson, Department of Anatomy, University of Mississippi Medical Center, 2500 North State Street, Jackson, MS 39216. Fax: 601-984-1655. E-mail: ksimpson@umc.edu

Received 21 June 2010; Accepted 13 November 2010

DOI 10.1002/ar.21350
Published online 8 September 2011 in Wiley Online Library (wileyonlinelibrary.com).

To visualize catecholamine neurons and their axons, earlier studies utilized the Falck-Hillarp method to reveal catecholamines in tissue sections by histofluorescence (Falck et al., 1962; Fuxe et al., 1968). These original studies were able to describe the extent of the noradrenergic (NE) cell bodies in the brainstem and extensive terminal fields throughout the neuraxis. More recently, immunohistochemical methods, based on the immunostaining of antibodies against either tyrosine hydroxylase (TH; the rate-limiting enzyme in catecholamine biosynthesis) and/or dopamine-β-hydroxylase (DBH; the final enzyme in norepinephrine biosynthesis), were introduced to reveal the expression of these markers not only within the locus coeruleus (LC) neurons but also the widespread NE fibers/axons nearly throughout the entire neuraxis (Hartman et al., 1972; Pickel et al., 1975; Hokfelt et al., 1976). More specifically, DBH is a widely used specific biomarker for NE cortical fibers. On the other hand, since TH is the first enzyme in the synthetic pathways of catecholamines, it has been commonly utilized to identify both the NE LC and dopaminergic (DA) substantia nigra and ventral tegmental area neurons.

Interestingly, previous studies in rats have found that TH immunoreactivity can be detected only in LC somata and their dendritic processes but not in NE LC axons; however, it can be expressed in both DA neurons and their axons (Pickel et al., 1975; Hokfelt et al., 1977). The lack of TH immunoreactivity in the NE nerve terminals, especially in the neocortex, has been suggested to be a consequence of rather low TH enzyme concentration in NE terminals compared to the much higher TH activity in DA axon terminals. Furthermore, the TH immunoreactive cortical fibers arising from DA neurons have been well documented to be restricted to cortical areas including four typical DA mesocortical regions: the medial frontal cortex, anterior cingulate cortex, entorhinal cortex, and perirhinal cortex (Hokfelt et al., 1977). Interestingly, TH immunoreactive fibers have been noted in neocortical areas of primates (Lewis et al., 1987). As their labeling pattern differed from the NE DBH immunoreactive fibers, the authors have inferred that such TH immunoreactive fibers were DA projections to the primate neocortex.

The locus coeruleus NE (LC-NE) system develops quite early and plays a regulatory role in brain development (Levitt and Moore, 1979). With respect to early development, several recent studies have reported that brain regions other than the LC, such as the neocortex, contain TH immunoreactive neurons (Satoh and Suzuki, 1990; Asmus et al., 2008). Further, Asmus et al., (2008) suggested that these transient TH expressing neurons were interneurons, because they can be double labeled with parvalbumin and calretinin antibodies. Unfortunately, the precise functional significance of these transiently TH expressing neurons in the neocortex remains to be elucidated.

Most of the previous studies have studied the LC-NE system by stressing adult animals (see review: Sabban and Kvetnansky, 2001), and very few, if any, have investigated this in neonates. The general conclusion derived from these studies is that the key event in response to stress is the persistent activation of TH expression in LC neurons. Moreover, this activation of TH expression in LC neurons depends on the duration and repetition of the stress. Interestingly, the changes of LC cortical fiber density may depend on the intensity of the stress. For example, repeated mild stress caused LC axonal sprouting (Nakamura, 1989, 1991; Sakaguchi et al., 1990) whereas severe stress triggered LC fiber's degeneration (Sakaguchi et al., 1990; Kitayama et al., 1994, 1997). In contrast, chronic exposure to antidepressants in adult rats tends to exert an opposite effect, that is, LC neurons are less excitable and with decreased expression of TH mRNA and protein (Nestler et al., 1990, 1999). Up to now, the effect of perinatal exposure to antidepressants on the TH expression in LC neurons, and their axon terminals is largely unknown.

Finally, several attempts have been made previously to use mutant mice to study pathophysiology during early development. For example, Levitt and Noebels (1981) reported that the mutant mouse "tottering" (tg) exhibited a twofold to threefold increase in the number of NE axons in nearly all the LC terminal fields compared with wild-type (WT) mice. This finding provided the first indication that gene-linked alteration of developmental events affects the NE system. In a subsequent study, Levitt (1988) further reported that such hyperinnervation in the "tottering" mouse was due to a direct genetic alteration of axon growth by LC neurons, rather than to selective shrinkage of targets in the presence of normal terminal arbors, because there was no obvious increase on the number of LC neurons between the mutants and WT mice. Monoamine oxidase A (MAO A) is a key enzyme to degrade serotonin and norepinephrine (Shih et al., 1999; Bortolato et al., 2008). Recently, a novel line monoamine oxidase A knock out (MAO A KO) mice was generated (Scott et al., 2008). These KO mice lack MAO A enzyme activity with increased level of serotonin and norepinephrine in the brain, and exhibit enhanced aggression toward intruder mice. At present, the consequence of such genetic manipulation on the NE system has yet to be explored.

In this report, we described altered TH expression in the NE system following perinatal exposure to selective serotonin reuptake inhibitor (SSRI) citalopram (CTM) in rat pups and in gene-linked (MAO A KO) mice. Specifically, double and/or triple immunohistochemical methods were conducted to characterize the abnormal distribution and their pathology of TH and DBH, as well as norepinephrine transporter (NET) expression in the LC, and their neocortical terminal fields from either CTM neonatally exposed rats or MAO A KO mice. A portion of these findings have been presented in preliminary form (Zhang et al., 2009).

MATERIALS AND METHODS

All procedures were approved by the University of Mississippi Medical Center Animal Care and Use Committee and complied with AAALAC and NIH guidelines. Rats were weaned at postnatal day (PN) 8 and housed in groups of 2–3/cage under standard laboratory conditions with *ad lib* access to food and water. After drug administration, rats were studied for a variety of behavioral tests and then sacrificed when they reached adulthood. As for the MAO A KO mice, they were generated in our laboratory (Jean C. Shih, University of Southern California) (Scott et al., 2008). All procedures were approved by the University of Southern California Animal Care and Use Committee and complied with AAALAC and NIH guidelines.

Treatment, Dosing, and Experimental Subsets

Shortly after the delivery of timed-pregnant Long Evans rats, the offspring were cross fostered to produce litters of 10–12 pups. The pups were tattooed for identification on PN6. Beginning on PN8, the pups were weighed and injected subcutaneously with CTM (10 mg/kg, Tocris, Ellisville, MO) or saline in a volume of 0.1 mL twice daily (total CTM dose of 20 mg/kg/day or saline volume of 0.2 mL/day) for 14 days (PN8-21). Additionally, a nontreatment subgroup (handled, but no drug injection was made) was also included as a group in our experimental study.

The CTM dose was selected to approximate the upper range of maternal and placental serum reported in clinical reports of maternal antidepressant treatment. This was more fully discussed in our previous reports (Maciag et al., 2006; Weaver et al., 2010). Subjects from each treatment group were then assigned to an experimental subset. One of the reasons for such case pairings was to permit simultaneous side by side evaluations of TH-immunostaining patterns. This allowed us to establish neurochemical differences among treatment groups. Tissue from one experimental subset (nontreatment, saline and CTM exposed), for example, was processed simultaneously (even in the same reaction chamber) and exposed to the same antiserum solutions to minimize staining variability. In current study, the comparison of TH immunoreactive fiber patterns in the rat was based on five male experimental subsets (totally 15 rats). As for the MAO A KO mice, a total of 22 male mice were used, among them, WT ($n = 4$ at day 30, and $n = 7$ at day 150), and MAO A KO ($n = 4$ at day 30, and $n = 7$ at day 150) mice.

Animal Sacrifice

After deeply anesthetized with Nembutal (75 mg/kg; i.p.), animals were perfused through the ascending aorta with saline first, followed by 3.5% paraformaldehyde in 0.1 M phosphate-buffered saline (PBS). The brains were removed and placed in the same fixative containing 25% sucrose overnight at 4°C. Brains were marked using small cut with a #10 blade. This procedure allowed us to later distinguish one animal from another.

Immunohistochemistry

To examine the effects of neonatal CTM exposure and genetic manipulation on TH expression in the neocortex, double and/or triple fluorescent immunohistochemical techniques were used. Brains were cut with an AO freezing microtome at 40 μm. The tissue was sectioned in the coronal plane, and permitted to freely float in small, individual wells with PBS. Sections were selected from tissue samples that were collected for each experimental subset. Areas of interest were identified in each case and a series of sections were chosen (typically three in every six sections). Keeping all tissue from an experimental subset together, sections were processed using anti-rabbit TH antibody (1:1000, Millipore, Temecula, CA) for 48 hr (24 hr at room temperature and then 24 hr at 4°C), followed by several rinses in PBS, and then incubated with a biotinylated anti-rabbit IgG (BA1000, ABC kit, Vector Laboratories, Burlingame, CA) for 1 hr at room temperature. Neuronal profiles were then visualized using Cy3-conjugated streptavidin (red, 1:200, Jackson Immunoresearch Laboratories, West Grove, PA) for 1 hr at room temperature in the dark. For double immunostaining, brain tissues were typically first processed for either anti-mouse DBH (1:1000, Millipore, Temecula, CA) or anti-mouse NET (1:1000, Mab, Stone Mountain, GA) for 48 hr. After several rinses in PBS, sections were then linked with a biotinylated anti-mouse IgG (BA9200, ABC kit, Vector Laboratories, Burlingame, CA) for 1 hr at room temperature. Neuronal profiles were then visualized using Cy2-conjugated streptavidin (green, 1:200, Jackson Immunoresearch Laboratories, West Grove, PA) for 1 hr at room temperature in the dark. After DBH or NET immunostaining, sections were rinsed and then incubated in anti-rabbit TH antibody (1:1000, Millipore, Temecula, CA) for 24 hr at 4°C followed by Cy3-conjugated anti-rabbit IgG (red, 1:200, Jackson Immunoresearch Laboratories, West Grove, PA) for 1 hr at room temperature in the dark. Furthermore, to assure that TH immunoreactive fibers in the rat and mouse brain tissues were not artifact from one source of antibody, several other sources of TH antibodies (e.g., anti-sheep TH or anti-mouse TH, Millipore, Temecula, CA) were also included. The immunostained patterns in our experimental brain tissues were rather identical across these antisera. To further assure that TH immunoreactive cortical axons were indeed NE, in some instances, a triple labeling strategy was conducted. Thus, anti-rabbit DBH, anti-mouse NET, and anti-sheep TH antibodies were utilized and then linked with their specific IgG and fluorescent tags (Cy5, Cy2, and Cy3, respectively). Finally, sections from the different cases/treatment groups were reassembled and mounted on gelatin-coated slides and then covered with DPX.

To control for nonspecific labeling, we conducted a set of experiments where sections were processed according to the protocol, except that the primary TH antiserum was omitted. Following this procedure, no immunoreactivity was detected. Further control studies, where an inappropriate secondary antibody was used for linkage, yielded the same (negative) result.

Data Analysis

To semiquantitatively analyze alterations in TH and/or DBH immunoreactivity density and intensity that were attributable to CTM treatment or genetic manipulation, digital photomicrographs of desired sections containing LC neurons and the neocortex were taken at a magnification of ×10 and ×20, respectively, using a Nikon E800 epifluorescent microscope. The ×20 magnification yielded 344 × 437 μm^2 terminal field area of the neocortex. For a given case, tissue sections from both sides of the LC and the neocortex (Paxinos and Watson, 1986; bregma at −3.3 mm) were photographed through each target area. Three images (for rats) and two images (for mice) were acquired from pia surface down to layer V as a cortical column, and four columns were photographed and analyzed from each hemisphere and both hemispheres were examined. As for the LC region, a ×10 objective was used and two to three sections at middle level of the LC were photographed and then analyzed. As for the pathological neuronal profiles, a ×40 objective was utilized.

To quantify the density of NE TH and/or DBH fibers in the neocortex, typically, the images were first

"flattened/skeletonized" to more readily distinguishable objects of interest from background distortions. A "thresholding" overlay was then applied to each image to delineate objects of interest (i.e., TH immunoreactive fibers). This utility specifies which information is to be extracted for measurement consideration. In the analysis of density, the "percentage of threshold area" was determined for each image. This measurement refers to the proportion of the entire digital image that was threshold.

As for the intensity measurement, the exposure time of each image was kept constant. The images were analyzed with MetaMorph Imaging software (Molecular Devices). These black and white images, that were pseudo-colored, encode intensity information pixel by pixel over a range (0–4095) of grayscale values. The stained intensity and density of a labeled profile was then measured using "show region statistics" tool. In this assay, stronger fluorescent signals (higher averaged gray values) point to higher level of protein expression. After thresholding the pictures, values of LC intensity as well as density were obtained. Values from each image were tabulated across sections and recorded as an average value for that region in that case.

The blocked analysis of covariance (ANCOVA) test and Post Hoc Bonferroni test were used for both rats and mice. P value less than 0.05 was considered to be significant.

RESULTS

Altered NE TH Immunoreactivity in the LC and Neocortex of Neonatal CTM Exposed Rats

In our earlier reports, we noted that perinatal exposure to CTM not only induced a dramatic reduction of enzymatic expression within the serotonergic raphe nuclear complex but also their axon density in the cortical target sites such as the medial prefrontal cortex, the somatosensory cortex and the hippocampus (Maciag et al., 2006; Weaver et al., 2010). Because CTM is considered one of highly SSRIs (Butler and Meegan, 2008), it is very likely that such treatment only selectively affects the serotonergic system. However, it is also known that biogenic amines neurochemically and anatomically interact among each other (Devau et al., 1987; Simpson and Lin, 2008). Thus, it is conceivable that such perinatal exposure to CTM may also affect other systems such as the NE circuitry.

The TH expression of LC neurons among three experimental groups (nontreatment, saline, and CTM exposed) were easily identified (Fig. 1A1–C1). Based on our semiquantitative analysis, there was no obvious difference (Fig. 1A2–C2) among the three groups in terms of their intensity (Fig. 2A; $F = 0.158$, $P = 0.857$) and density (Fig. 2B; $F = 0.554$, $P = 0.602$). As for the dendritic morphology of individual TH immunoreactive LC neurons, most of them exhibited rather smooth processes (Fig. 1A3–C3), and this characteristic can also be demonstrated as a continuous band utilizing the "intensity profile" function of MetaMorph software program (Fig. 1A4–C4).

As for the TH immunoreactive fiber distribution in the neocortex, a consistent finding is that very few, if any, TH immunoreactive fibers were noted in nontreatment animals (Fig. 3A1), providing further support for the lack of TH immunoreactive fibers in the normal adult rodent neocortex reported previously. In contrast, a slight increased density of TH immunoreactive fibers was found in saline-exposed animals, and such increased expression of TH immunoreactive fibers in the neocortex was very noticeable in CTM exposed animals (Fig. 3B1 and C1). To assure that these TH immunoreactive fibers in the neocortex are indeed NE in origin, double immunofluorescent method utilizing both TH and DBH antibodies were conducted (Fig. 3A2–C2). The merged photos (Fig. 3A3–C3) clearly revealed such coexpression in all three experimental groups, suggesting the NE LC origin rather than the DA origin. The semiquantitative data revealed that the average threshold TH immunoreactive area (Mean ± SD) in nontreatment animals was 0.5% ± 0.3%, the saline-exposed animals was 0.8% ± 0.4%, and CTM-exposed animals was 1.9% ± 0.9% (Fig. 4A). Statistical analysis revealed that there was no significant difference between nontreatment and saline-exposed rats as for the density of NE TH immunoreactive fibers ($P = 0.774$); however, the density of NE TH immunoreactive fibers was more significantly increased in CTM-exposed rats compared with saline-exposed rats ($P = 0.023$) or nontreatment rats ($P = 0.004$). Thus, a ~twofold increase of the NE TH immunoreactive fibers was found in saline-exposed animals, and a nearly fourfold increase was observed in CTM-exposed animals compared with nontreatment animals.

Additionally, very few, if any, thick TH immunoreactive fibers were noted in nontreatment rats (Fig. 5A1 and C1). A slightly increased density of thick TH immunoreactive fibers was noted in saline-exposed rats (Fig. 5C2). Moreover, more thick TH immunoreactive fibers were noted in the neocortex of CTM-exposed rats compared with saline-exposed rats (Fig. 5C3). Interestingly, a few NE TH immunoreactive fibers showed beaded morphology in some CTM-exposed rats (Fig. 5B1). Again, these altered TH immunoreactive axons coexpressed DBH immunoreactivity (Fig. 5A2 and B2), confirming their NE LC origin (Fig. 5A3 and B3). The schematic diagrams illustrating the relative increased density and morphological changes among the three experimental groups were shown in Fig. 5.

To further understand the difference between the density of TH and DBH immunoreactive fibers in the neocortex, we also semiquantitatively analyzed the density of DBH immunoreactive fibers in nontreatment, saline-exposed rats, and CTM-exposed rats. Our data revealed that the density of DBH immunoreactive fibers (Mean ± SD) was: 5.6% ± 0.9% in nontreatment group, 5.2% ± 0.6% in saline-exposed group, and 5.6% ± 0.6% in CTM-exposed group (Fig. 4B). Statistical analysis did not show significant difference among three groups ($F = 0.326$, $P = 0.732$). These data suggest that early drug exposure does not appear to affect the overall DBH immunoreactive NE cortical fiber density.

Altered NE TH Immunoreactivity in the LC and Neocortex of MAO A KO Mice

Because MAO A KO mice contain extreme high levels of both serotonin and norepinephrine (Cases et al., 1995; Scott et al., 2008), it is conceivable that such a long-lasting high concentration of norepinephrine during early brain development may alter the expression of NE fibers in MAO A KO mice. Therefore, our goal, here, was to

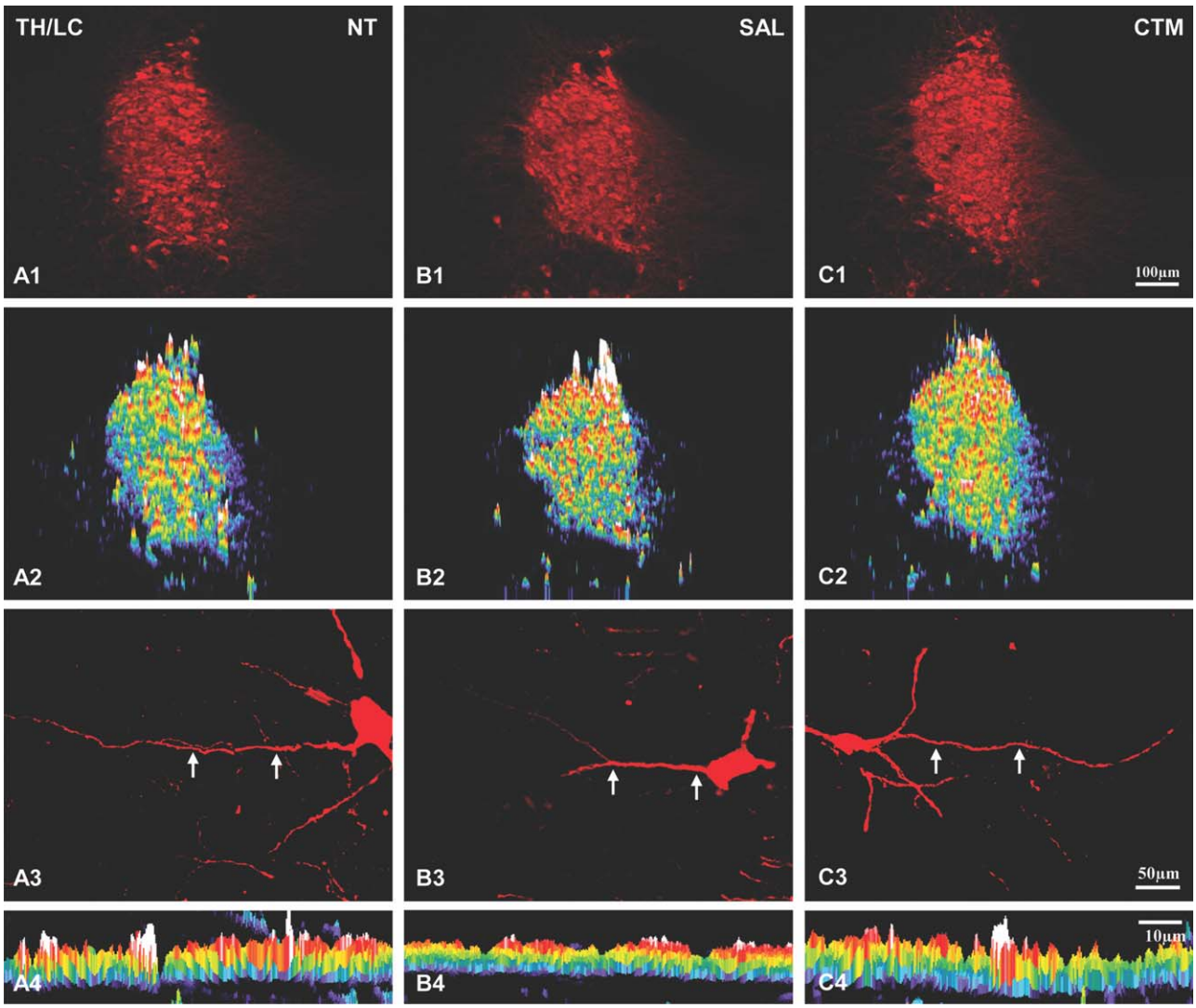

Fig. 1. Expression profiles of TH immunoreactivity in the LC of nontreatment (NT), saline (SAL), and CTM exposed rats. Intensity profiles of TH immunostained LC are shown in **A2** (NT), **B2** (SAL), and **C2** (CTM). Note no apparent staining intensity (white represents highest intensity; purple represents lowest intensity) differences among the three groups of animals. High power view of individual TH immunoreactive LC neurons and their dendrites are shown in **A3**, **B3**, and **C3**. The dendritic TH intensity profile and its spatial distribution are shown in **A4**, **B4**, and **C4**. Note the expanded view (pointed by two arrows in A3, B3, and C3) of TH immunostained dendrite reveals a continuous band of activity and also exhibits rather similar intensity. Scale bar in **C1** applies to **A1** and A2 rows. Scale bar in C3 applies to A3 row. Scale bar in C4 applies to A4 row.

examine the morphological changes of NE neocortical fibers labeling patterns at day 30 and 150. An example of TH expression in LC neurons was shown in Fig. 6. First, there were no obvious changes both in the intensity (Fig. 7A, $F = 0.171$, $P = 0.72$) and density (Fig. 7B, $F = 0.044$, $P = 0.853$) of TH expression between WT and MAO A KO mice at day 30, and also there were no obvious changes both in the intensity (Fig. 7A, $F = 0.625$, $P = 0.487$) and density (Fig. 7B, $F = 1.846$, $P = 0.267$) of TH expression between WT and MAO A KO mice at day 150. However, on further examination of the TH-labeled LC dendrites in MAO A KO mice, we noted that many LC neurons exhibited beaded dendrites, especially at day 30 (Fig. 6B3) compared with day 150 (Fig. 6C3). In contrast, LC neurons in WT mice exhibited rather smooth dendrites (Fig. 6A3). More specifically, MetaMorph software morphological analysis revealed rather segregated immunoreactivity in segments of LC dendrites in MAO A KO mice at day 30 (Fig. 6B4) and day 150 (Fig. 6C4), compared with the almost even (smooth) TH immunoreactivity in WT LC dendrites (Fig. 6A4).

As LC neurons revealed abnormal dendritic morphology, it is very likely that axons of their target sites such as the neocortex may also exhibit altered morphology. To test this, we utilized antibodies against TH and NET to examine the axonal terminal morphology and their density in the neocortex. Based on our semiquantitative analysis of TH immunoreactive fiber density in the neocortex, our data revealed that the average threshold TH

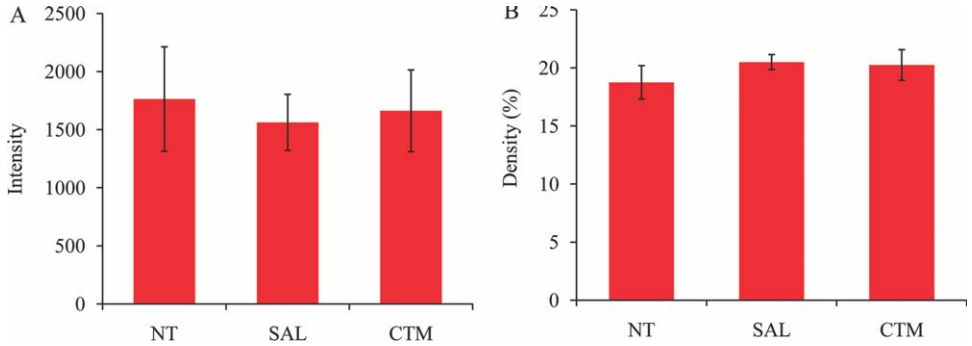

Fig. 2. Histograms demonstrating the intensity (**A**) and density (**B**) of TH immunoreactivity in the LC. All three experimental groups showed a rather similar intensity and density.

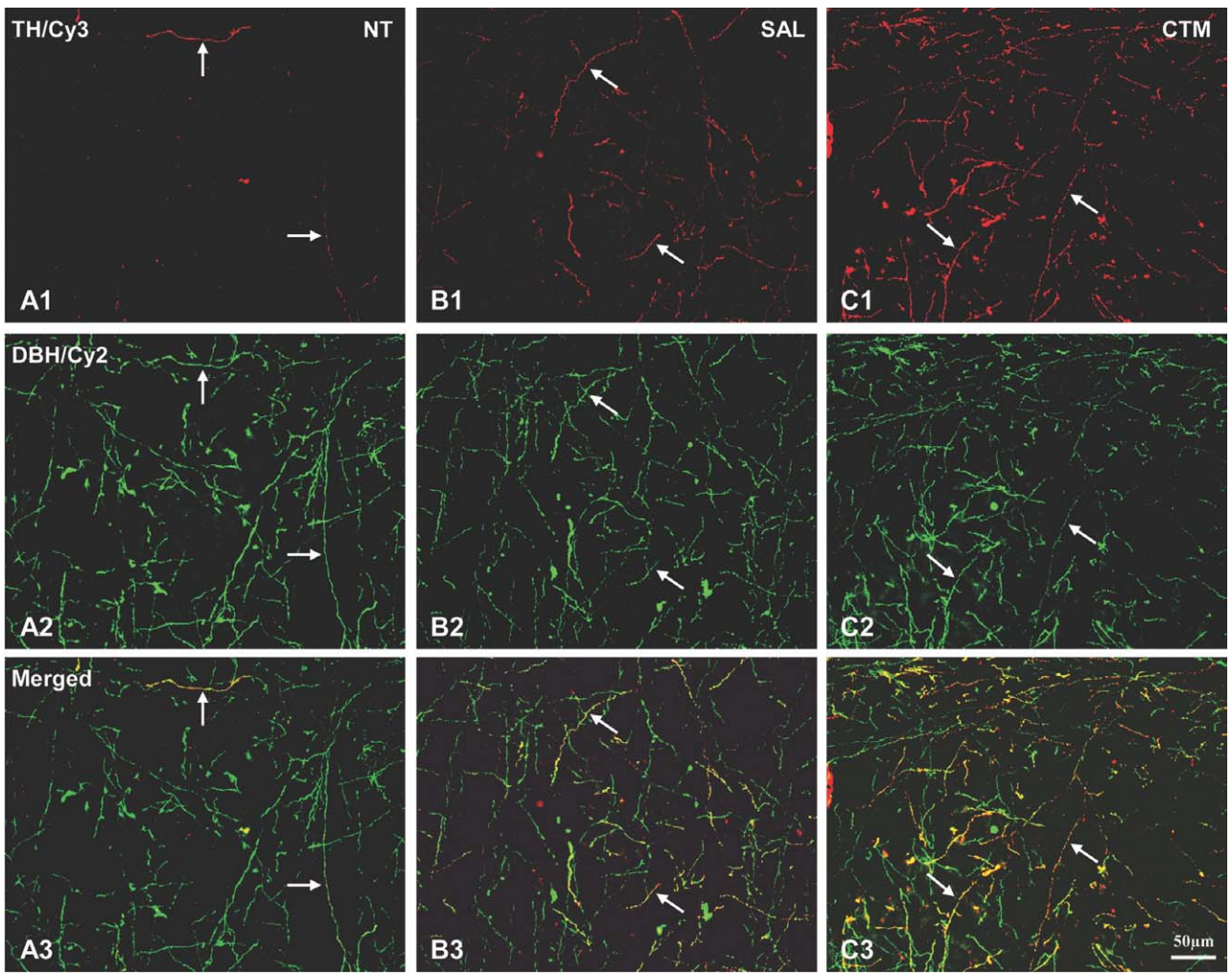

Fig. 3. The immunostaining patterns of NE TH immunoreactive neocortical fibers in rats. Note the increase of NE TH immunoreactive cortical fiber density (linked to Cy3: red) in SAL (**B1**) and CTM (**C1**) exposed animals compared to NT (**A1**) animals. The same tissues were also processed for DBH immunorectivity (**A2**, **B2**, and **C2**; linked to Cy2: green). Notice the TH immunoreactive fibers coexpress DBH immunoreactivity (pointed by white arrows). The merged images are shown in **A3**, **B3**, and **C3**. Numerous TH/DBH double labeled fibers are observed in CTM-exposed animals (C3) compared with NT (A3). Scale bar in C3 applies to all images.

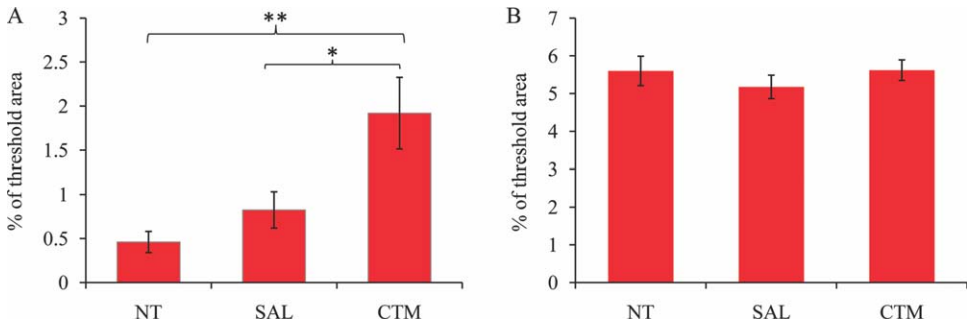

Fig. 4. Histograms demonstrating alterations of TH (**A**) and DBH (**B**) immunoreactive fiber density in rat neocortex among the three experimental groups. (*$P < 0.05$, **$P < 0.01$).

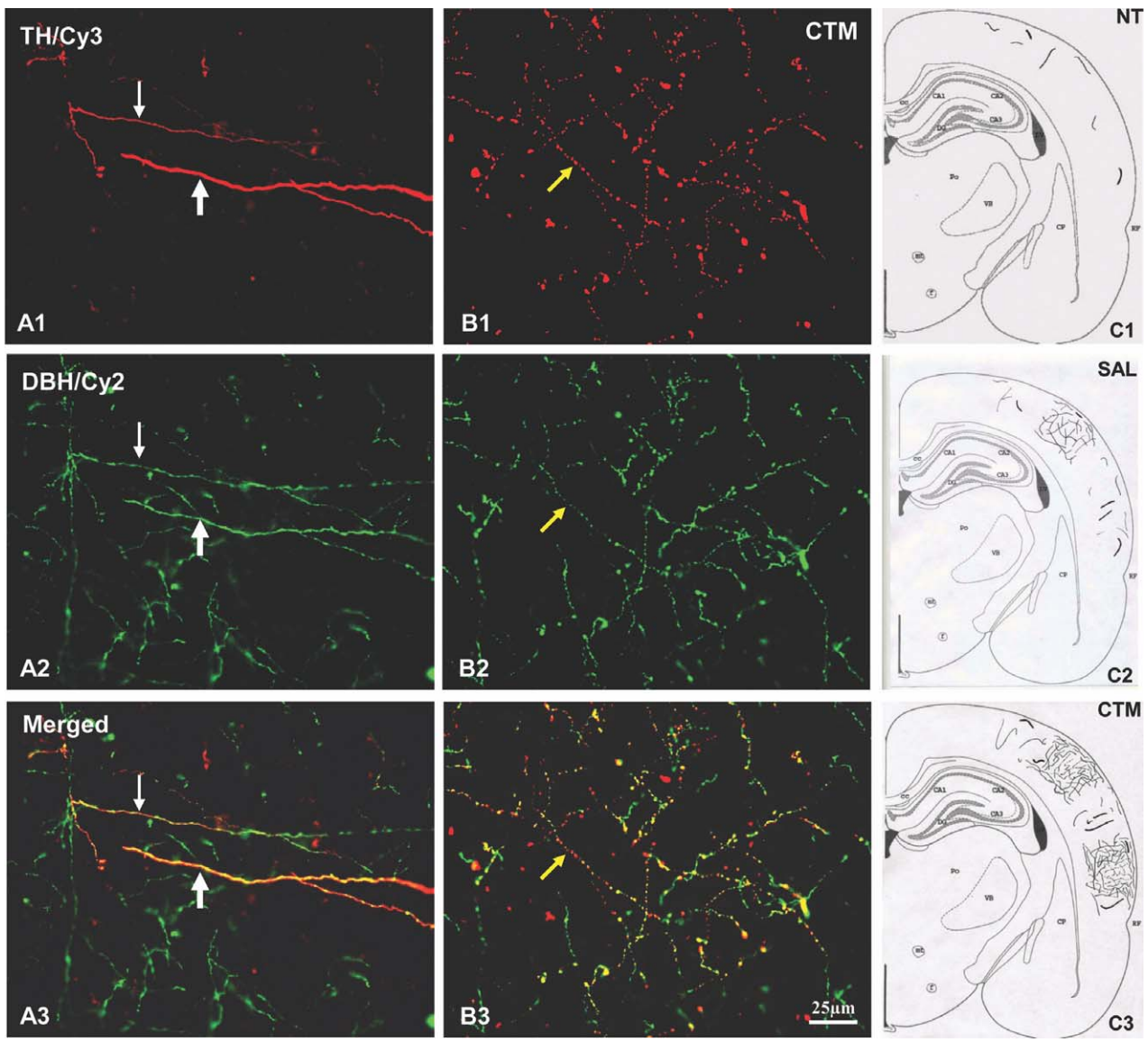

Fig. 5. Representative extra-thick (hypertrophy) NE TH immunoreactive fibers and the overall distribution of NE TH immunoreactive fibers in rat neocortex. A few extra-thick TH immunoreactive fibers (linked to Cy3; pointed by thick white arrow in **A1**) in all rats especially CTM-exposed rats are noted to coexpress DBH immunoreactivity (linked to Cy2, see **A2**). The merged image is shown in **A3**. For comparison, thin white arrows point to regular fine NE TH immunoreactive fibers. Interestingly, clusters of fine caliber NE TH immunoreactive fibers exhibit beaded appearance in some CTM-exposed animals (pointed by yellow arrows). The merged image is shown in **B3**. Schematic diagrams illustrating the overall distributions of NE TH immunoreactive fibers among the three groups are shown in **C1**, **C2**, and **C3**. Note especially, the clustering of NE TH immunoreactive fibers in the CTM-exposed animals. Scale bar in B3 applies to all the color photos.

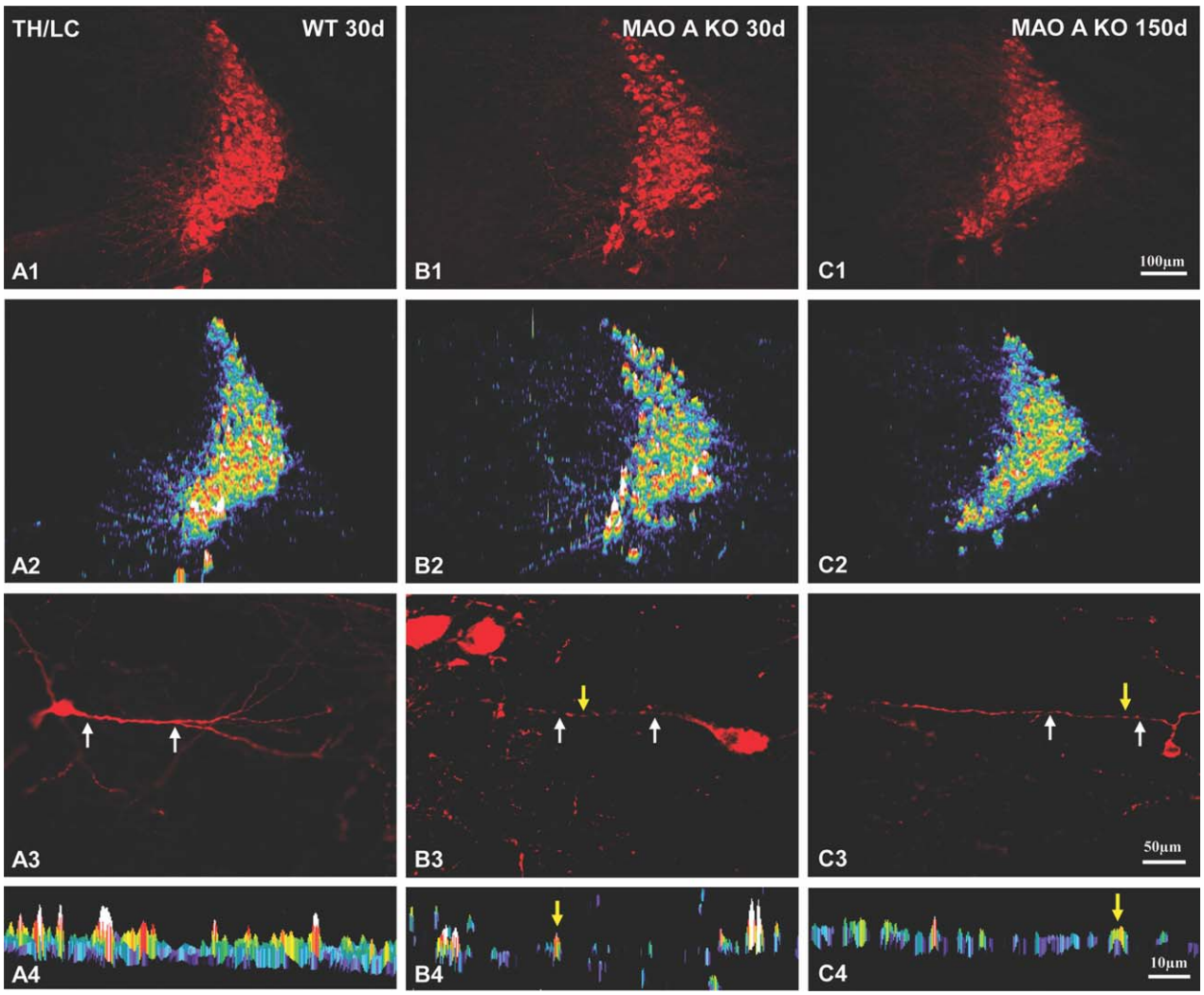

Fig. 6. Expression profiles of TH immunoreactivity in the LC of MAO A KO (day 30 and 150) and WT (day 30) mice. Note the rather similar intensity profiles of TH immunreactivity among the three groups of animals in **A2**, **B2**, and **C2**. High power views of individual TH immunoreactive LC neurons are shown in **A3**, **B3**, and **C3**. The intensity and spatial distribution profiles of TH immunoreactive dendrites (pointed by two white arrows in A3, B3, and C3) are shown in **A4**, **B4**, and **C4**. Yellow arrows represent the "beaded appearance" profiles in B3, C3, B4, and C4. Notice especially the beaded appearance of dendrites in MAO A KO mice at day 30 (B4) compared with day 150 (C4). In contrast, rather smooth dendrites are often found in WT (A4). Scale bar in **C1** applies to **A1** and A2 rows. Scale bar in C3 applies to A3 row. Scale bar in C4 applies to A4 row.

immunoreactive cortical fiber area in WT mice (Mean ± SD) was 1.4% ± 0.2% compared to 1.9% ± 0.5% in MAO A KO mice at day 30 (Fig. 7C, $F = 2.28$, $P = 0.228$). As for day 150 old mice, we noted that the average threshold area (Mean ± SD) was 3.4% ± 0.6% in WT mice compared to 3.1% ± 0.5% in MAO A KO mice (Fig. 7C, $F = 0.411$, $P = 0.55$). These data demonstrate a slight increase of TH immunoreactive cortical fiber density in MAO A KO mice compared with WT mice at younger age but appears to subside when the animals reached adulthood. Furthermore, NE TH immunoreactive cortical fibers in WT mice are double labeled with NET immunoreactivity, and they are rather smooth, suggesting the LC as their cell origin (Fig. 8A1–A4). Interestingly, the TH/NET double-labeled neocortical axonal terminals were found to be rather beaded in MAO A KO mice at day 30 (Fig. 8B1–B4), and slightly beaded at day 150 (Fig. 8C1–C4) compared to smooth axons in WT mice. In addition, such alteration/beading appeared to be more obvious in TH expressing axons (Fig. 8B2), especially at day 30, compared with NET expressing axons (Fig. 8B4).

DISCUSSION

The results of the present investigation reveal that neonatal exposure to one of the most selective SSRIs, CTM, increases NE TH expression in rat neocortex. In particular, we conducted double and/or triple immunofluorescent techniques to assure that these TH expressing fibers/axons in the cortical hemispheres are indeed NE.

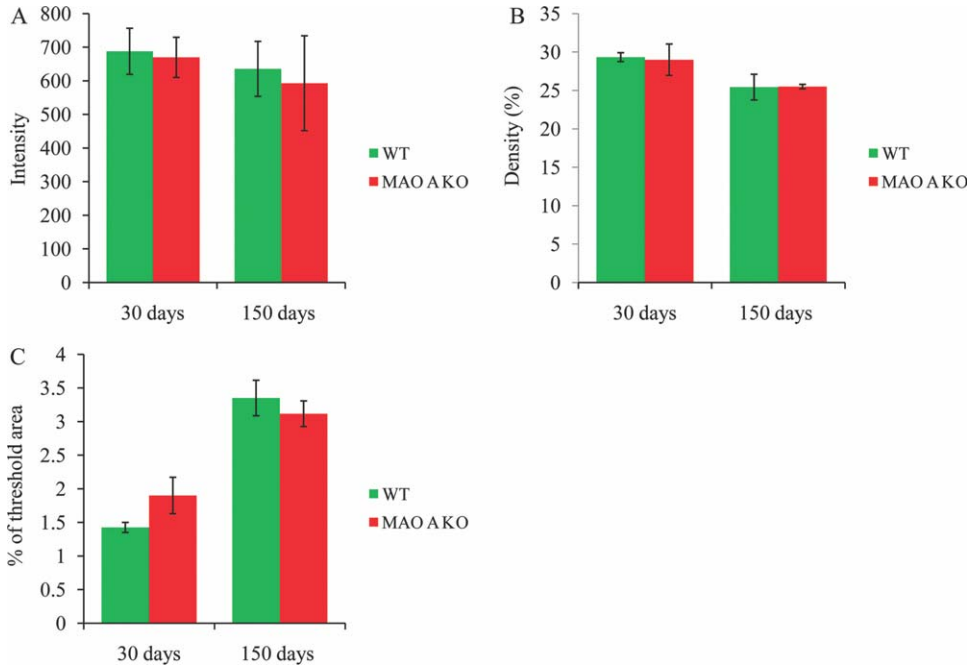

Fig. 7. Histograms demonstrating the alterations of TH expression intensity and density in the LC as well as TH immunoreactive cortical fiber density in 30 and 150 days old WT and MAO A KO mice. **A**: TH expression intensity of the LC remained unchanged in MAO A KO mice compared with WT mice at both ages. **B**: TH expression density of the LC also remained unchanged in MAO A KO mice compared with WT mice at both ages. **C**: The density of NE TH immunoreactive fibers in MAO A KO mice was slightly higher at day 30 ($P = 0.228$) but remained unchanged at day 150 ($P = 0.55$) compared with WT mice, respectively.

Furthermore, MAO A KO mice exhibited TH expressing beaded dendrites of LC neurons compared with the smooth LC dendrites in WT mice. A slightly increased density of NE TH expressing cortical fibers with varicosities was also observed in MAO A KO mice compared with the rather smooth TH expressing NE axons in WT mice. Taken together, our present findings suggest that enhanced NE TH expression in rodent neocortex can be induced by manipulating the levels of biogenic amines, most notably serotonin, either through drug exposure during early development or genetic means.

Technical Considerations

In the current experiments, double and/or triple fluorescent immunohistochemical techniques were conducted to reveal the altered NE TH expressing fibers in rodent neocortical hemispheres. As it is well known that specificity of the antibodies may slightly differ from one antibody to another, we have addressed this issue by utilizing three different sources of TH antibodies. Our data revealed a consistent pattern of enhanced NE TH expressing fibers in the neocortex regardless of the type of antibody used following either drug exposure during early development or genetic manipulation.

Furthermore, immunohistochemical staining pattern may vary slightly from one animal to another depending on the conditions in which it is performed. To avoid such variation, animals were perfused on the same day, sectioned also on the same day, and then the brain sections from three experimental groups were processed simultaneously together as a set in the same well/container. With such approach, comparison between cases in the same set revealed consistently, for example, an increased density of NE TH expressing fibers in the neocortex following CTM exposure compared with either nontreatment or saline-exposed animals.

Changes in the density of NE TH expressing cortical fibers were analyzed using semiquantitative immunofluorescent technique. More specifically, MetaMorph software program allows us to optimally sample the labeled fibers within the selected area. To avoid sampling bias, four columns of each cortical hemisphere (two hemispheres per animal) were conducted. This allows us to perform a rather detailed analysis among different experimental groups. Most importantly, semiquantitative analysis of immunostained fiber density has been recently utilized by several laboratories including ours (Dreyer et al., 2004; Maciag et al., 2006; Weaver et al., 2010). One of the major advantages with this approach is that changes on the immunostained profiles within a subzone/subregion of a given area/nucleus can be analyzed. Such approach cannot be easily achieved with Western blot analysis.

Comparison With Other Studies

Previous studies have suggested that very few, if any, TH expressing fibers were found in the normal adult rodent (especially the rat) neocortex (Pickel et al., 1975; Hokfelt et al., 1977). In our TH-immunostained materials obtained from nontreatment or WT groups, a consistent finding was that there were only a few TH immunoreactive fibers in rodent neocortex, supporting

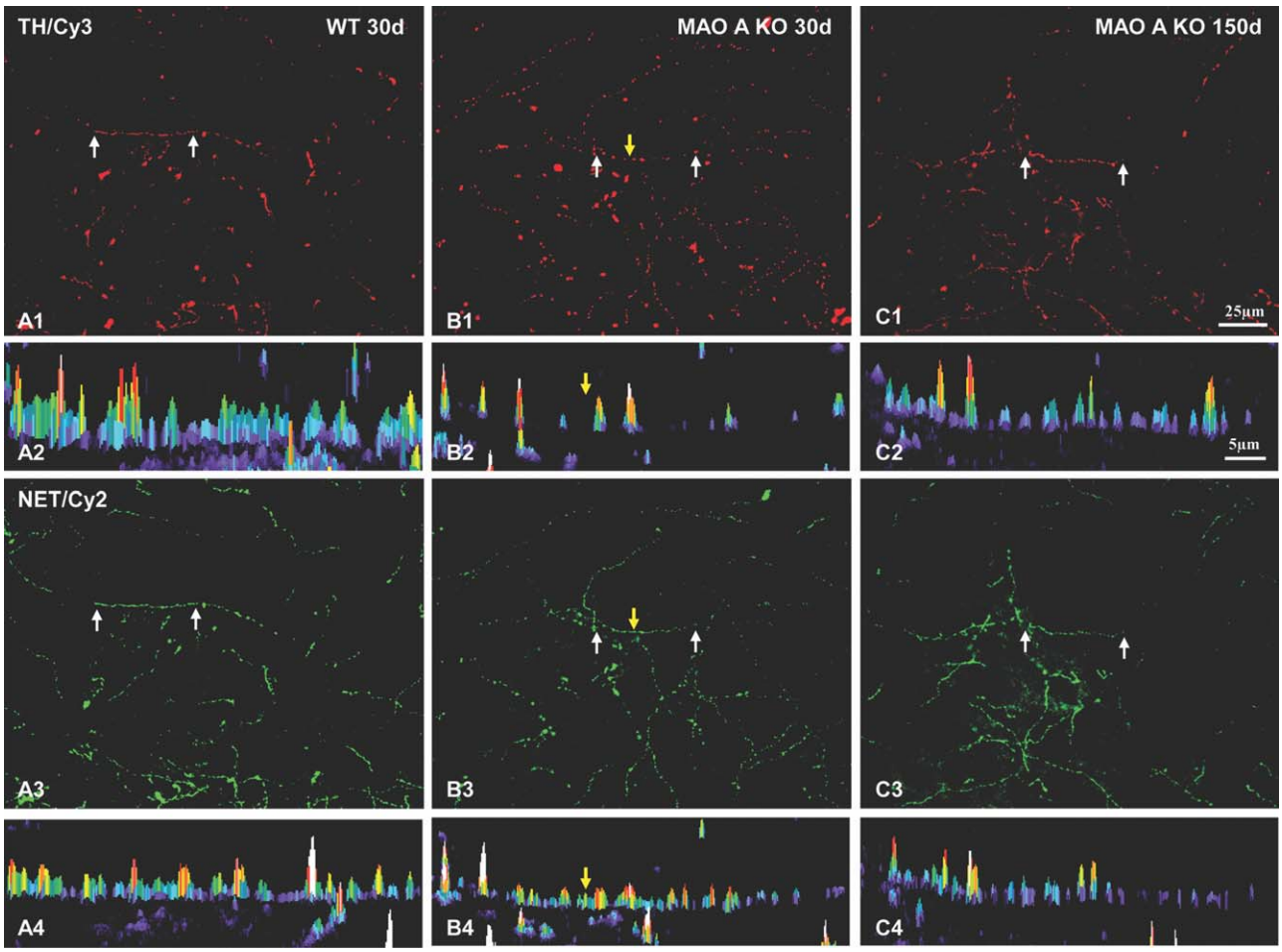

Fig. 8. The intensity and spatial profiles of NE TH immunoreactive fibers in WT and MAO A KO mice. Notice especially the beaded appearance of TH immunoreactive cortical fibers in MAO A KO mice at day 30 (**B1**) compared with day 150 (**C1**). Rather continuous labeling patterns are found in WT (**A1**). The spatial and intensity profiles of TH immunoreactivity from a segment (pointed by two white arrows in A1 row) of three groups are shown in **A2** row, respectively. Nearly all TH immunoreactive fibers (linked to Cy3: red) coexpress NET immunoreactivity (linked to Cy2: green). The spatial and intensity profiles of NET immunoreactivity from a segment (pointed by two white arrows in **A3** row) of three groups are shown in **A4** row, respectively. Interestingly, segregations of NET immunoreactive fibers (**B4**) in MAO A KO mice at day 30 are not as obvious as NE TH immunoreactive fibers (**B2**). Yellow arrows point to the "gap" between two "beaded appearance" profiles in B1 column. Scale bar in C1 applies to A1 and A3 rows. Scale bar in **C2** applies to A2 and A4 rows.

the overall conclusions derived from the previous reports especially the rat. So far, few studies have examined the altered NE TH expressing cortical fibers following various types of manipulation in neonates. In contrast, there are numerous examples of altered TH expression (both the protein and mRNA levels), especially in LC neurons, after stressing the adult animals (Richard et al., 1988; Watanabe et al., 1995; Chang et al., 2000). Other study has further shown that not only TH but also the biosynthetic enzyme such as DBH protein and mRNA levels were also increased in the LC after immobilization stress (Serova et al., 1999). Furthermore, several reports have shown that stressful experience can reduce NE axon density in the cortex (Sakaguchi et al., 1990; Kitayama et al., 1994, 1997). These two lines of evidence suggest that stress may lead to an increased expression of TH/DBH in LC neurons but a corresponding reduction of NE cortical fiber density. One of the current intriguing findings is that neonatal exposure to saline slightly enhanced NE TH immunoreactive cortical fiber density compared with nontreatment. One possible explanation is that rat pups may have also responded to stress during saline administration, such as maternal separation or injection discomfort. Further experiments are certainly needed to properly elucidate such possible mechanism(s).

So far, most of the antidepressant treatment studies have been conducted in adult animals and the analysis was restricted to LC neurons. For example, Nestler et al., (1990) reported that chronic antidepressant (all major classes of antidepressant medication) administration decreased (40%–70%) the expression of TH in rat LC neurons. The decreased level of TH immunoreactivity corresponded to the decrease of TH mRNA levels. On the other hand, Nakamura (1990) reported that infusion of the antidepressants maprotiline or desipramine into

the adult rat cortex pretreated with catecholamine neurotoxin 6-hydroxydopamine induced regeneration of NE cortical axon terminals, suggesting potent norepinephrine reuptake inhibitors can alter the distribution of NE axons in the cerebral hemispheres. Furthermore, Kitayama et al., (1997) also reported that antidepressant imipramine promoted the regeneration of NE axons. Unfortunately, very few, if any, studies have addressed the effect of NE axons in the neocortex after neonatal exposure to antidepressants such as SSRIs. Nonetheless, it seems likely that antidepressant exposure to adults but not neonates may increase the density of NE axons in the neocortical hemispheres, whereas antidepressant exposure to neonates may increase the density and alter the morphology of NE TH immunureactive fibers in the neocortex. Furthermore, we have noted also a rather similar upregulation of NE TH immunoreactive fibers in animals exposed to CTM from PN1-10 (data not shown). These lines of evidence imply further that manipulation of serotonin level during early brain development may alter the function of the NE system.

It is also intriguing to note that interaction between serotonergic and NE cortical axons appears to exist (see brief review: Harley, 2003). For example, Liu et al. (2003) reported that regeneration of NE axons in adult rat cortex was impeded by the presence of normal serotonergic fibers. The authors further demonstrated that regeneration of serotonergic fibers occurred much faster than NE axons after neurotoxin damage. Because our recent studies have also demonstrated that neonatal exposure to CTM decreased the serotonergic (immunostained with serotonin transporter SERT antibody) cortical fiber density (Maciag et al., 2006; Weaver et al., 2010), our present data further support the notion of a compensatory interaction between serotonergic and NE systems.

A previous study has shown the appearance of abnormally enlarged (hypertrophic) TH immunoreactive fibers in the hippocampus after a selective norepinephrine neurotoxin DSP-4 exposure (Booze et al., 1988). Interestingly, perinatal CTM exposure also induced the appearance of a few extra-thick (hypertrophic) NE TH expressing cortical axons. Needless to say, further investigations are required to determine whether these abnormally enlarged cortical axons are indeed functionally normal.

Given the fact that "tottering" mutant mice exhibited a pronounced hyperinnervation of NE axons in the cortex (Levitt, 1988), it is not surprising for us to note that genetic manipulation of MAO A also induces a slightly enhanced density of NE TH expressing axons in MAO A KO mice compared with WT mice. However, our data also revealed that dendrites of LC neurons in MAO A KO mice are rather beaded, suggesting a sign of partial degeneration. In addition, we have also noted that NE TH expressing cortical axons exhibited varicosities/beading in MAO A KO mice compared with the rather smooth axons in WT mice. The current findings also lead us to believe that the altered NE system in MAO A KO mice may not function properly, because previous studies have demonstrated that mild transient ischemic insult induces dendritic beading of hippocampal pyramidal cells (Lin et al., 1997; Simpson and Lin, 2002).

It is worth pointing out that despite a few rather thick or beaded looking NE TH immunoreactive fibers in the neocortex of CTM-exposed rats, the majority of these NE TH immunoreactive fibers are still smooth. In previous reports, we also found that there are some thick or beaded looking serotonergic fibers in CTM-exposed rats (Maciag et al., 2006; Weaver et al., 2010). These two lines of data appear to support the notion that thick or beaded looking fibers may be the result of pathological changes of axon terminals.

Functional Significance

Perhaps, the most intriguing point of the current study is the upregulation of NE TH expressing fibers in the neocortex after perinatal manipulation either via drug exposure or gene mutation. For example, about 0.5%, 0.8%, and 1.9% of NE TH immunoreactive fibers were found in nontreatment, saline- and CTM-exposed animals, respectively. Interestingly, the density of DBH immunoreactive cortical fibers was not changed among the three groups (5.6% in nontreatment group). This data confirmed an early report of about 5.5% regarding the density of DBH immunoreactive cortical fibers in normal rats (Kitayama et al., 1994). To estimate the percentage of these NE TH immunoreactive fibers out of DBH immunoreactive fibers in the three experimental groups, we recalculated our data, thus, in the normal condition about 8.7% of the NE cortical fibers expressed TH immunoreactiviy, whereas almost 33% of NE cortical fibers expressed TH immunoreactiviy in CTM-exposed animals. At present, it remains to be elucidated why only about one-third of the NE system appears to be upregulated in CTM-exposed animals.

It is interesting to note that previous studies have suggested a raphe-derived inhibitory action of serotonin on TH activity in LC neurons (Lewis et al., 1976; McRae-Degueurce et al., 1982; Devau et al., 1987). For example, Sturtz et al., (1994) noticed an increased TH activity and TH mRNA of the LC after administration of 5,6-dihydroxytryptamine, a neurotoxin known to selectively destroy serotonergic neurons. Haddjeri et al., (1997) also reported that lesion of serotonin neurons resulted in enhanced LC firing rate. Recently, it was reported that the tryptophan hydroxylase immunoreactivity, the rate-limiting enzyme of serotonin biosynthesis, was reduced in neonatal CTM-exposed rats (Maciag et al., 2006). Hence, SSRI exposure during development may produce a serotonergic lesion-type effect, resulting in increased expression of TH in the LC-NE system.

As increased LC activity, which results in increased extracellular norepinephrine level, was noted under fear or anxiety condition (Mason and Fibiger, 1979; Redmond and Huang, 1979; Weiss et al., 2005), it is possible that enhanced TH expression in LC axons, which results in enhanced synthesis of norepinephrine in LC axons, may also contribute to the anxiety-like behaviors of perinatal SSRIs-exposed animals (Ansorge et al., 2004, 2008).

Finally, there are numerous lines of evidence that implicate the heterogeneous uptake among biogenic amines (Feuerstein et al., 1986; Descarries et al., 1987; Vizi et al., 2004; Zhou et al., 2005). Utilizing NET KO mice as their experimental model, Vizi et al., (2004) reported that norepinephrine can be taken up and released by serotonin varicosities. The authors further suggested that the diffusion of norepinephrine may be spatially limited by SERTs. Unfortunately, the coexpression of norepinephrine and serotonin within the same axons in these

NET KO mice was not addressed. Under the same scenario, the CTM (despite its selectivity) may, thus, enhance not only serotonergic but also NE neurotransmission. We have, in fact, explored such a possibility in our experimental model. Our data (data not shown) suggested that none of the SERT immunoreactive cortical fibers coexpress TH and/or DBH immunoreactivity, suggesting an unlikely release of norepinephrine from SERT immunoreactive cortical axons in our experimental model. Finally, our current data revealed an enhanced NE TH expression following perinatal exposure to CTM, suggesting strongly the intimate interaction between the two systems, regardless of the selectivity of SSRIs during early brain development.

At present, SSRIs are the first-line drug choice dealing with major depressive disorders especially during pregnancy and lactation. Our finding suggests that perinatal SSRIs exposure may have the potential to alter the LC-NE neuronal circuitry later in life. Hence, clinicians should weigh the pros and cons of prescribing SSRIs to pregnant and nursing mothers.

ACKNOWLEDGEMENTS

The authors thank Loai Alzghoul for help with the immunohistochemical staining, Nidhi Khatri for drug administration, and Warren May for statistical analysis.

LITERATURE CITED

Ansorge MS, Morelli E, Gingrich JA. 2008. Inhibition of serotonin but not norepinephrine transport during development produces delayed, persistent perturbations of emotional behaviors in mice. J Neurosci 28:199–207.

Ansorge MS, Zhou M, Lira A, Hen R, Gingrich JA. 2004. Early-life blockade of the 5-HT transporter alters emotional behavior in adult mice. Science 306:879–881.

Asmus SE, Anderson EK, Ball MW, Barnes BA, Bohnen AM, Brown AM, Hartley LJ, Lally MC, Lundblad TM, Martin JB, Moss BD, Phelps KD, Phillips LR, Quilligan CG, Steed RB, Terrell SL, Warner AE. 2008. Neurochemical characterization of tyrosine hydroxylase-immunoreactive interneurons in the developing rat cerebral cortex. Brain Res 1222:95–105.

Booze RM, Hall JA, Cress NM, Miller GD, Davis JN. 1988. DSP-4 treatment produces abnormal tyrosine hydroxylase immunoreactive fibers in rat hippocampus. Exp Neurol 101:75–86.

Bortolato M, Chen K, Shih J. 2008. Monoamine oxidase inactivation: from pathophysiology to therapeutics. Adv Drug Deliv Rev 60:1527–1533.

Butler SG, Meegan MJ. 2008. Recent developments in the design of anti-depressive therapies: targeting the serotonin transporter. Curr Med Chem 15:1737–1761.

Cases O, Seif I, Grimsby J, Caspar P, Chen K, Pournin S, Muller U, Aguet M, Babinet C, Shih JC, Maeyer ED. 1995. Aggressive behavior and altered amounts of brain serotonin and norepinephrine in mice lacking MAOA. Science 268:1763–1766.

Chang MS, Sved AF, Zigmond MJ, Austin MC. 2000. Increased transcription of the tyrosine hydroxylase gene in individual locus coeruleus neurons following footshock stress. Neuroscience 101:131–139.

Descarries L, Lemay B, Doucet G, Berger B. 1987. Regional and laminar density of the dopamine innervation in adult rat cerebral cortex. Neuroscience 21:807–824.

Devau G, Multon MF, Pujol JF, Buda M. 1987. Inhibition of tyrosine hydroxylase activity by serotonin in explants of newborn rat locus ceruleus. J Neurochem 49:665–670.

Dreyer J, Schleicher M, Tappe A, Schilling K, Kuner T, Kusumawidijaja G, Müller-Esterl W, Oess S, Kuner R. 2004. Nitric oxide synthase (NOS)-interacting protein interacts with neuronal NOS and regulates its distribution and activity. J Neurosci 24:10454–10465.

Falck B, Hillarp NA, Thieme G, Torp A. 1962. Fluorescence of catecholamines and releated compounds condensed with formaldehyde. J Histochem Cytochem 10:348–354.

Feuerstein TJ, Hertting G, Lupp A, Neufang B. 1986. False labelling of dopaminergic terminals in the rabbit caudate nucleus: uptake and release of [3H]-5-hydroxytryptamine. Br J Pharmacol 88:677–684.

Fuxe K, Hamburger B, Hokfelt T. 1968. Distribution of noradrenaline nerve terminals in cortical areas of the rat. Brain Res 8:125–131.

Haddjeri N, Claude de Montigny, Pierre Blier. 1997. Modulation of the firing activity of noradrenergic neurons in the rat locus coeruleus by the 5-hydroxytrptamine system. Br J Pharmacol 120:865–875.

Harley CW. 2003. Norepinephrine and serotonin axonal dynamics and clinical depression: a commentary on the interaction between serotonergic and noradrenergic axons during axonal regeneration. Exp Neurol 184:24–26.

Hartman BK, Zide D, Udenfriend S. 1972. The use of dopamine β-hydroxylase as a marker for the central noradrenergic nervous system in rat brain. Proc Nat Acad Sci USA 69:2722–2726.

Hokfelt T, Johansson O, Fuxe K, Goldstein M, Park D. 1976. Immunohistochemical studies on the localization and distribution of monoamine neuron systems in the rat brain. I. Tyrosine hydroxylase in the mes- and diencephalon. Med Biol 54:427–453.

Hokfelt T, Johansson O, Fuxe K, Goldstein M, Park D. 1977. Immunohistochemical studies on the localization and distribution of monoamine neuron systems in the rat brain II. Tyrosine hydroxylase in the telencephalon. Med Biol 55:21–40.

Kitayama I, Nakamura S, Yaga T, Murase S, Nomura J, Kayahara T, Nakano K. 1994. Degeneration of locus coeruleus axons in stress-induced depression model. Brain Res Bull 35:573–580.

Kitayama I, Yaga T, Kayahara T, Nakano K, Murase S, Otani M, Nomura J. 1997. Long-term stress degenerates, but imipramine regenerates, noradrenergic axons in the rat cerebral cortex. Biol Psychiatry 42:687–696.

Levitt P. 1988. Normal pharmacological and morphometric parameters in the noradrenergic hyperinnervated mutant mouse, "tottering." Cell Tissue Res 252:175–180.

Levitt P, Moore RY. 1979. Development of the noradrenergic innervation of neocortex. Brain Res 162:243–259.

Levitt P, Noebels JL. 1981. Mutant mouse tottering: selective increase of locus coeruleus axons in a defined single-locus mutation. Proc Natl Acad Sci USA 78:4630–4634.

Lewis BD, Renaud B, Buda M, Pujol JF. 1976. Time-course variations in tyrosine hydroxylase activity in the rat locus coeruleus after electrolytic destruction of the nuclei raphe dorsalis or raphe centralis. Brain Res 108:339–349.

Lewis DA, Campbell MJ, Foote SL, Goldstein M, Morrison JH. 1987. The distribution of tyrosine hydroxylase-immunoreactive fibers in primate neocortex is widespread but regionally specific. J Neurosci 7:279–290.

Lin RCS, Matesic DF, Connor JA. 1997. The role of dendritic dysfunction in neurodegeneration. Ann N Y Acad Sci 825:134–145.

Liu Y, Ishida Y, Shinoda K, Nakamura S. 2003. Effects of repeated stress on regeneration of serotonergic and noradrenergic axons in the cerebral cortex of adult rats. Neurosci Lett 339:227–230.

Maciag D, Simpson KL, Coppinger D, Lu Y, Wang Y, Lin RCS, Paul IA. 2006. Neonatal antidepressant exposure has lasting effects on behavior and serotonin circuitry. Neuropsychopharmacology 31:47–57.

Mason ST, Fibiger HC. 1979. Current concepts. I. Anxiety: the locus coeruleus disconnection. Life Sci 25:2141–2147.

McRae-Degueurce A, Berod A, Mermet A, Keller A, Chouvet G, Joh TH, Pujol JF. 1982. Alterations in tyrosine hydroxylase activity elicited by raphe nuclei lesions in the rat locus coeruleus:

evidence for the involvement of serotonin afferents. Brain Res 235:285–301.
Nakamura S. 1990. Antidepressants induce regeneration of catecholaminergic axon terminals in the rat cerebral cortex. Neurosci Lett 111:64–68.
Nakamura S. 1991. Axonal sprouting of noradrenergic locus coeruleus neurons following repeated stress and antidepressant treatment. In: Barnes CD, Pompeiano O, editors. Neurobiology of the locus coeruleus: progress in brain research. Amsterdam: Elsevier Science Publishers B.V. p 587–598.
Nakamura S, Sakaguchi T, Aoki F. 1989. Electrophysiological evidence for terminal sprouting of locus coeruleus neurons following repeated mild stress. Neurosci Lett 100:147–152.
Nestler EJ, Alreja M, Aghajanian GK. 1999. Molecular control of locus coeruleus neurotransmission. Soc Biol Psychiatry 46:1131–1139.
Nestler EJ, Mcmahon A, Sabban EL, Tallman JF, Duman RS. 1990. Chronic antidepressant administration decreases the expression of tyrosine hydroxylase in the rat locus coeruleus. Proc Natl Acad Sci USA 87:7522–7526.
Paxinos G, Watson C. 1986. The rat brain in stereotaxic coordinates. 2nd ed. Sydney: Academic press.
Pickel VM, Joh TH, Reis DJ. 1975. Ultrastructural localization of tyrosine hydroxylase in noradrenergic neurons of brain. Proc Nat Acad Sci USA 72:659–663.
Redmond DE Jr, Huang YH. 1979. Current concepts. II. New evidence for a locus coeruleus-norepinephrine connection with anxiety. Life Sci 25:2149–2162.
Richard F, Faucon-Biguet N, Labatut R, Rollet D, Mallet J, Buda M. 1988. Modulation of tyrosine hydroxylase gene expression in rat brain and adrenals by exposure to cold. J Neurosci Res 20:32–37.
Sabban EL, Kvetnanský R. 2001. Stress-triggered activation of gene expression in catecholaminergic systems: dynamics of transcriptional events. Trends Neurosci 24:91–98.
Sakaguchi T, Nakamura S. 1990. Duration-dependent effects of repeated restraint stress on cortical projections of locus coeruleus neurons. Neurosci Lett 118:193–196.
Satoh J, Suzuki K. 1990. Tyrosine hydroxylase-immunoreactive neurons in the mouse cerebral cortex during the postnatal period. Dev Brain Res 53:1–5.
Scott AL, Bortolato M, Chen K, Shih JC. 2008. Novel monoamine oxidase A knock out mice with human-like spontaneous mutation. Mol Neurosci 19:739–743.
Serova LI, Nankova BB, Feng Z, Hong JS, Hutt M, Sabban EL. 1999. Heightened transcription for enzymes involved in norepinephrine biosynthesis in the rat locus coeruleus by immobilization stress. Biol Psychiatry 45:853–862.
Shih JC, Chen K, Ridd M. 1999. Monoamine oxidases: from genes to behavior. Ann Rev Neurosci 22:197–217.
Simpson KL, Lin RCS. 2002. Cellular and molecular mechanisms of ischemic tolerance. In: Lin RCS, editor. New concepts in cerebral ischemia. Boca Raton: CRC Press. p 263–306.
Simpson KL, Lin RCS. 2008. Neuroanatomical and chemical orgaization of the locus coeruleus. In: Ordway GA, Schwartz MA, Frazer A, editors. Brain norepinephrine: neurobiology and therapeutics. New York: Cambridge University Press. p 9–52.
Sturtz F, Rollet D, Faucon Biguet N, Mallet J, Buda M. 1994. Long-term alteration in rat tyrosine hydroxylase mRNA levels in locus coeruleus after intraventricular injection of 5,6-dihydroxytrptamine. Brain Res Mol Brain Res 22:107–112.
Vizi ES, Zsilla G, Caron MG, Kiss JP. 2004. Uptake and release of norepinephrine by serotonergic terminals in norepinephrine transporter knock-out mice: implications for the action of selective serotonin reuptake inhibitors. J Neurosci 24:7888–7894.
Watanabe Y, McKittrick CR, Blanchard DC, Blanchard RJ, McEwen BS, Sakai RR. 1995. Effects of chronic social stress on tyrosine hydroxylase mRNA and protein levels. Brain Res Mol Brain Res 32:176–180.
Weaver KJ, Paul IA, Lin RCS, Simpson KL. 2010. Neonatal exposure to citalopram selectively alters the expression of the serotonin transporter in the hippocampus: dose-dependent effects. Anat Rec 293:1920–1932.
Weiss JM, Boss-Williams KA, Moore JP, Demetrikopoulos MK, Ritchie JC, West CHK. 2005. Testing the hypothesis that locus coeruleus hyperactivity produces depression-related changes via galanin. Neuropeptides 39:281–287.
Zhang J, Ryan DD, Thaggard DD, Paul IA, Simpson KL, Lin RCS. 2009. Neonatal exposure to antidepressants alters developing serotonin and dopamine systems in rats. Program No. 436.14. 2009 Neuroscience Meeting Planner. Chicago, IL; Society for Neuroscience, 2009. Online.
Zhou FM, Liang Y, Salas R, Zhang L, De Biasi M, Dani JA. 2005. Corelease of dopamine and serotonin from striatal dopamine terminals. Neuron 46:65–74.